JOURNAL OF MATERIALS SCIENCE 21 (1986) 1786–1792

Laser pulse crystallization of Pd–Si metallic glasses

A. CALKA*, A. P. RADLIŃSKI
Department of Solid State Physics, Research School of Physical Sciences, Australian National University, Canberra ACT 2601, Australia

A novel method of laser pulse crystallization (LPC) capable of revealing and quantifying crystallization in amorphous ribbons is presented. It is used to study the morphology of crystallization and, indirectly, surface crystallization (SC) of Pd–Si amorphous alloys in the composition range $Pd_{77}Si_{23}$–$Pd_{85}Si_{15}$. The laser-induced, frozen-in fronts of crystallization are studied by optical metallography and X-ray diffraction. The shapes of these fronts are determined by the initial degree of SC, which depends on alloy compositions, their thermal history and/or the surface of the ribbon being analysed. SC is inactive in alloys of eutectic composition ($Pd_{85}Si_{15}$) and is most pronounced for compositions near the border to the amorphous region on the silicon-rich side ($Pd_{77}Si_{23}$). For as-quenched ribbons, a stronger tendency to SC exists on the shiny surface of the ribbon. Low-temperature furnace annealing as well as room temperature ageing over a period of 2 years equalizes the degree of SC on both surfaces. The X-ray diffraction patterns taken from the regions containing frozen-in fronts of crystallization only reveal the presence of metastable phase II, independently of composition and/or thermal history of the given sample.

1. Introduction

Metallic glasses have been studied extensively for over 15 years and have proved to be very attractive materials with extensive potential applications. Despite the great number of papers devoted to their study, many aspects of their properties still escape complete description. One of the main problems is irreproducibility of their properties. Owing to their sensitivity to the details of casting conditions and their thermal history, amorphous alloys of the same chemical compositions, and obtained with apparently identical melt-spinning techniques, may exhibit different physical and chemical properties. This work provides evidence that the source of these difficulties lies in their surface condition, which is characterized by the concentration of the nucleation sites quenched-in during the casting process and/or precipitated due to heat treatment or ageing. Some of these inhomogeneities catalyse heterogeneous crystallization of columnar crystals growing from the surface into the bulk of the amorphous ribbons. Hence, the microstructure of crystallized ribbons sometimes reflects their initial surface condition.

The successful growth of columnar crystals reported so far in the literature required isothermal annealing well below the crystallization temperature during a suitably long period of time [1]. Such a crystallization technique unavoidably activates diffusion and relaxation processes and, therefore, affects the intrinsic properties of the ribbon under study. In this work we present a novel laser pulse crystallization (LPC) method which is quick and capable of revealing crystallization morphology and, indirectly, the surface condition of amorphous ribbons.

2. Experimental methods

The crystallization of amorphous ribbons studied here was induced by depositing thermal energy contained in a single shot of 512 nm (green) argon ion laser radiation. The best results are obtained with a pulse duration of 1 sec at a power level of 3 to 5 W.

The beam was focused on a ribbon with a 25mm focal length cylindrical lens in such a manner that the long axis of the resulting narrow, high intensity light strip (being the image of the laser output coupler) was perpendicular to the long axis of the ribbon (Fig. 1). In most of our experiments the ribbons were suspended in air. As the result of the laser shot, the sample was locally heated, heat flow occurred in both directions out of the illuminated region and crystallization took place along the sample. The fast-moving front of crystallization was eventually frozen-in in that part of the ribbon where the temperature dropped below the temperature of crystallization. The time necessary for this to take place was of the order of seconds. Such a short duration of the crystallization process effectively eliminates relaxation as well as diffusion of the amorphous structure. Thus, the microstructure of the ribbon as well as the shape of the frozen-in front of crystallization reflect properties of the amorphous ribbon as chacterized prior to the laser annealing experiment. This is in contrast to the furnace annealing results, which are inherently affected by evolution of the ribbon properties during the annealing.

* *Permanent address*: Institute of Materials Science and Engineering, Warsaw Technical University, Poland.

0022–2461/86 $03.00 + .12

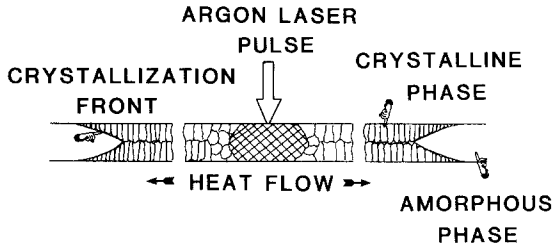

Figure 1 Principle of the laser pulse crystallization (LPC) method.

For this experiment Pd–Si amorphous alloys were specifically chosen because, although they have been one of the metallic glasses investigated most intensively for the last 15 years, there are many remaining discrepancies about their stability and crystallization mechanisms. Pd–Si master alloys, composed of high purity elements, were melted in evacuated fused quartz capsules. Amorphous ribbons of compositions $Pd_{85}Si_{15}$, $Pd_{80}Si_{20}$ and $Pd_{77}Si_{23}$ were obtained by rapid quenching from the melt by means of the single roller melt-spinning method (copper roller). After verifying by X-ray diffraction that the ribbons were completely amorphous they were crystallized using the LPC method described above. All samples were investigated as follows: (i) in the as-quenched state, (ii) after isothermal pre-annealing at 335° C for 5 min, (iii) after pre-annealing as above and consecutive chemical etching, and (iv) after ageing for 2 years at room temperature.

X-ray diffraction patterns were taken from both shiny and mat surfaces with a computerized quantitative X-ray diffraction system. X-ray patterns were taken within the range 20° to 160° using Co$K\alpha$ radiation. Throughout this paper, only fragments of X-ray patterns including the first amorphous peak are presented. For the phase determination, a complete set of data from the computer storage was used.

3. Results and discussion

3.1. $Pd_{77}Si_{23}$ alloys

Fig. 2 shows the frozen-in fronts of crystallization of the $Pd_{77}Si_{23}$ amorphous ribbons: (a) as-quenched state (ribbon thickness $\sim 18\,\mu$m); (b) as-quenched state (ribbon thickness $\sim 27\,\mu$m); (c) pre-annealed (335° C for 5 min); (d) aged at room temperature, and (e) chemically etched after pre-annealing.

Fig. 3 shows X-ray diffraction patterns taken from both surfaces of ribbons in some of these states prior to LPC.

Optical metallography of the as-quenched thin ribbons reveals the crystallization of cellular crystals grown from both surfaces. The X-ray diffraction patterns taken before crystallization from both surfaces show only "ideally" bell-shaped broad peaks corresponding to the amorphous structure.

The metallography of the as-quenched thicker ribbons (thickness $\sim 27\,\mu$m) reveals that the crystallization process starts from the shiny surface. The growth of columnar crystals from this surface into the bulk is clearly seen. A characteristic asymmetry of the growth process with respect to the two surfaces of the ribbon is observed. Taking into account that (1) the observed front of crystallization is more advanced from the shiny surface side, and (2) that at distances far from the point of original laser irradiation the temperature of the ribbon at a given distance is a decreasing function of time, we may conclude that the more stable cooling surface is depleted of quenched-in sites that constitute the driving force of crystallization.

The X-ray diffraction pattern taken from the shiny surface of the thicker ribbon (Fig. 3a) does not show clearly the existence of crystalline phases, but some structure on the amorphous peak close to the peak positions of metastable phase I (MSI) [2] and crystalline palladium is observed. The shapes of the LPC fronts of the ribbon pre-annealed for 5 min at 335° C, as well as those aged at room temperature for 2 years,

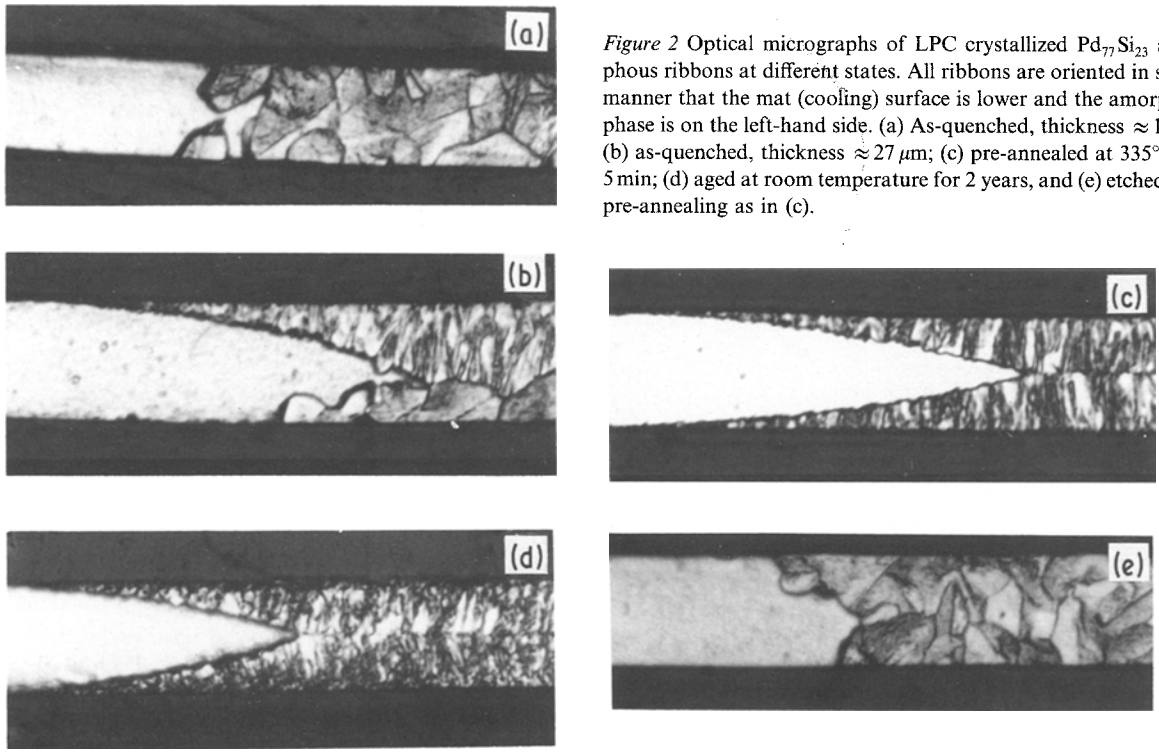

Figure 2 Optical micrographs of LPC crystallized $Pd_{77}Si_{23}$ amorphous ribbons at different states. All ribbons are oriented in such a manner that the mat (cooling) surface is lower and the amorphous phase is on the left-hand side. (a) As-quenched, thickness $\approx 18\,\mu$m; (b) as-quenched, thickness $\approx 27\,\mu$m; (c) pre-annealed at 335° C for 5 min; (d) aged at room temperature for 2 years, and (e) etched after pre-annealing as in (c).

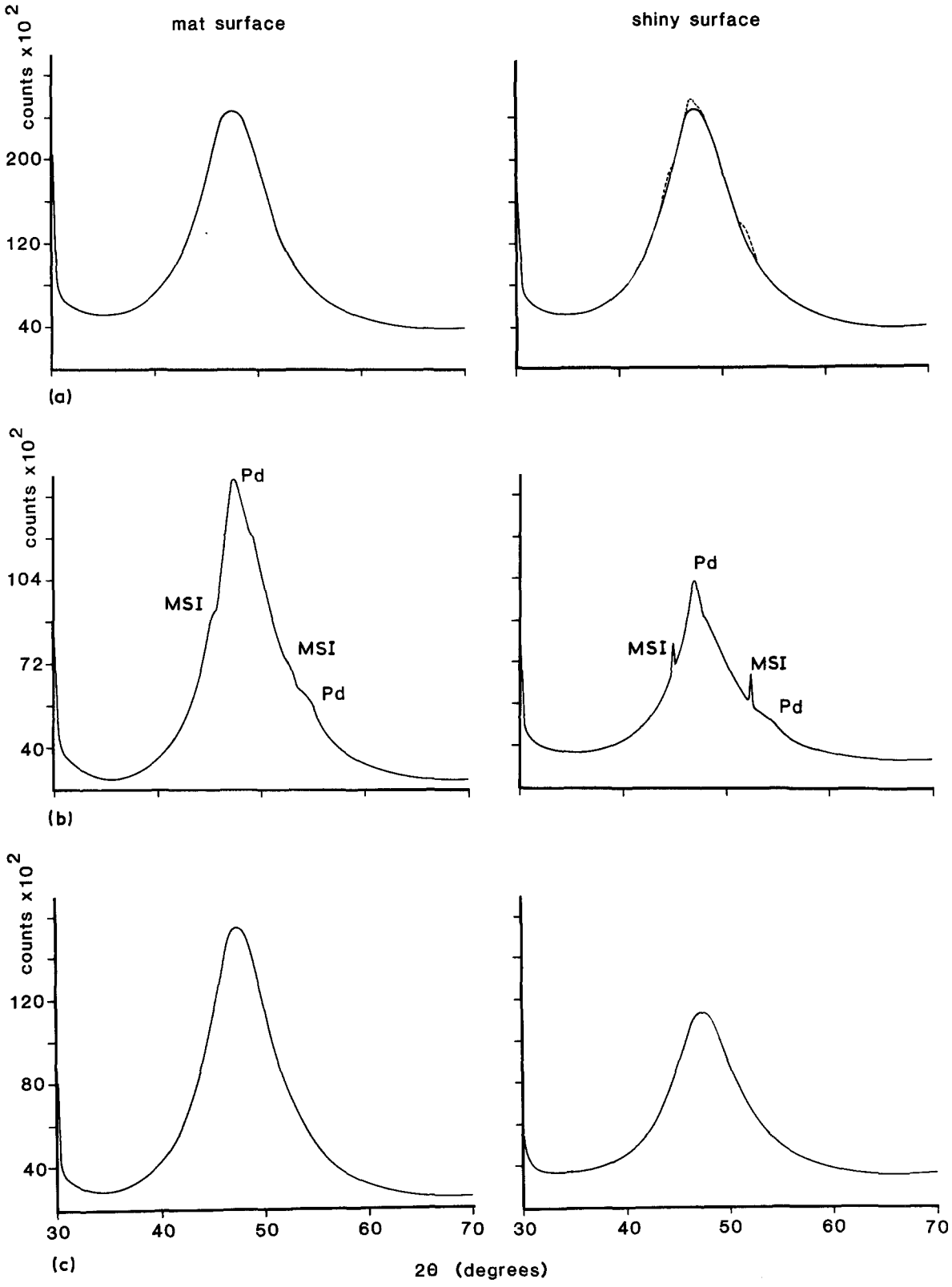

Figure 3 X-ray patterns taken from both surfaces of $Pd_{77}Si_{23}$ amorphous ribbons prior to LPC. (a) As-quenched, (b) pre-annealed at 335° C for 5 min, and (c) etched after pre-annealing.

are distinctly different (Fig. 2c, d). A symmetrical frontal growth of columnar crystals from both surfaces is observed. This result might indicate that the annealing equalizes the number of nucleation sites on both surfaces. It also means that the heat flow along the ribbon is homogeneous despite the fact that all laser radiation was absorbed practically on one surface only.

The X-ray diffraction patterns taken from surfaces of pre-annealed samples are presented in Fig. 3b. The shapes of those two X-ray diffraction patterns correspond to the same phases: amorphous + Pd + MSI. The only difference between them is that the crystalline components of the X-ray patteren taken from the shiny surface are more pronounced, with the peaks of MSI and Pd phases clearly seen. In contrast, the X-ray pattern taken from the mat surface reveals a much more washed-out structure characteristic of the phases MSI and Pd. It is due to very small size of the microcrystallites present on the mat surface.

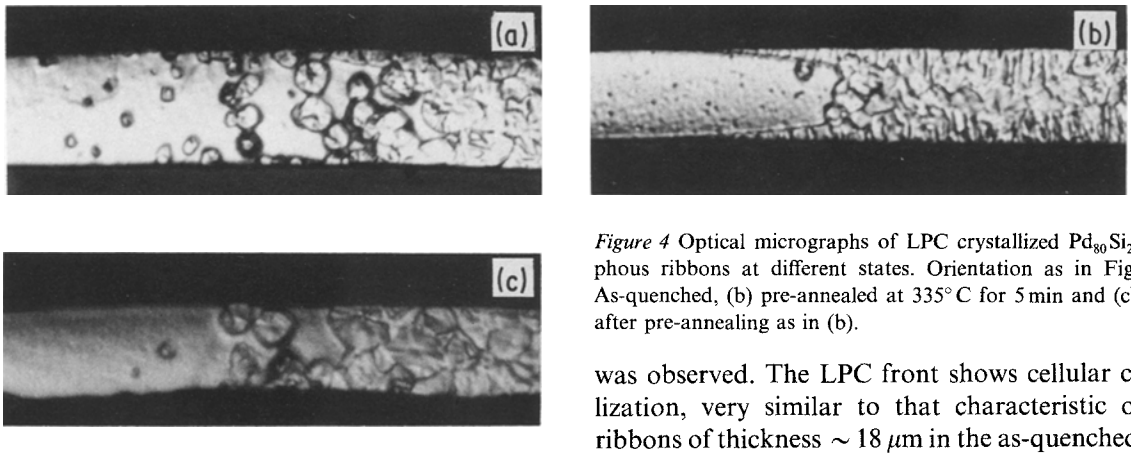

Figure 4 Optical micrographs of LPC crystallized $Pd_{80}Si_{20}$ amorphous ribbons at different states. Orientation as in Fig. 2. (a) As-quenched, (b) pre-annealed at 335° C for 5 min and (c) etched after pre-annealing as in (b).

As described by Masumoto and Maddin [2], the MSI had an fcc structure with lattice constant $a = 0.407$ nm. In the angular region containing the first amorphous peak only the MSI (1 1 1) and (2 0 0) lines are located (Figs 3, 5 and 7). To fully identify the MSI additional diffraction peaks occurring in the region $70° \leqslant 2\theta \leqslant 160°$ were also used. These peaks have been identified as Pd (2 2 2), (3 1 1) and MSI (2 2 0), (3 1 1) reflexes.

Fig. 3e shows X-ray diffraction patterns taken from the chemically etched surfaces of pre-annealed samples. A layer of thickness approximately 1 μm was etched off from both surfaces. The X-ray diffraction patterns for both surfaces now reveal a fully amorphous structure, with the "ideal" shape of the broad peak corresponding to the amorphous phase. For such prepared samples, no columnar crystallization was observed. The LPC front shows cellular crystallization, very similar to that characteristic of thin ribbons of thickness ~ 18 μm in the as-quenched state. This result clearly indicates that columnar crystallization is induced by crystallites pre-existing on both surfaces.

3.2. $Pd_{80}Si_{20}$

The result of the LPC presented in Fig. 4a indicates that, for as-quenched ribbons, homogeneous crystallization to spherical crystals takes place. Such a microstructure can be achieved only under the influence of exclusively bulk crystallization mechanisms. Surface processes are not active here, probably due to the absence of relevant nucleation sites for this particular ribbon composition.

The X-ray diffraction patterns taken from both surfaces of as-quenched $Pd_{80}Si_{20}$ ribbons show a fully amorphous structure with the "ideal" shape of the amorphous peak (Fig. 5a).

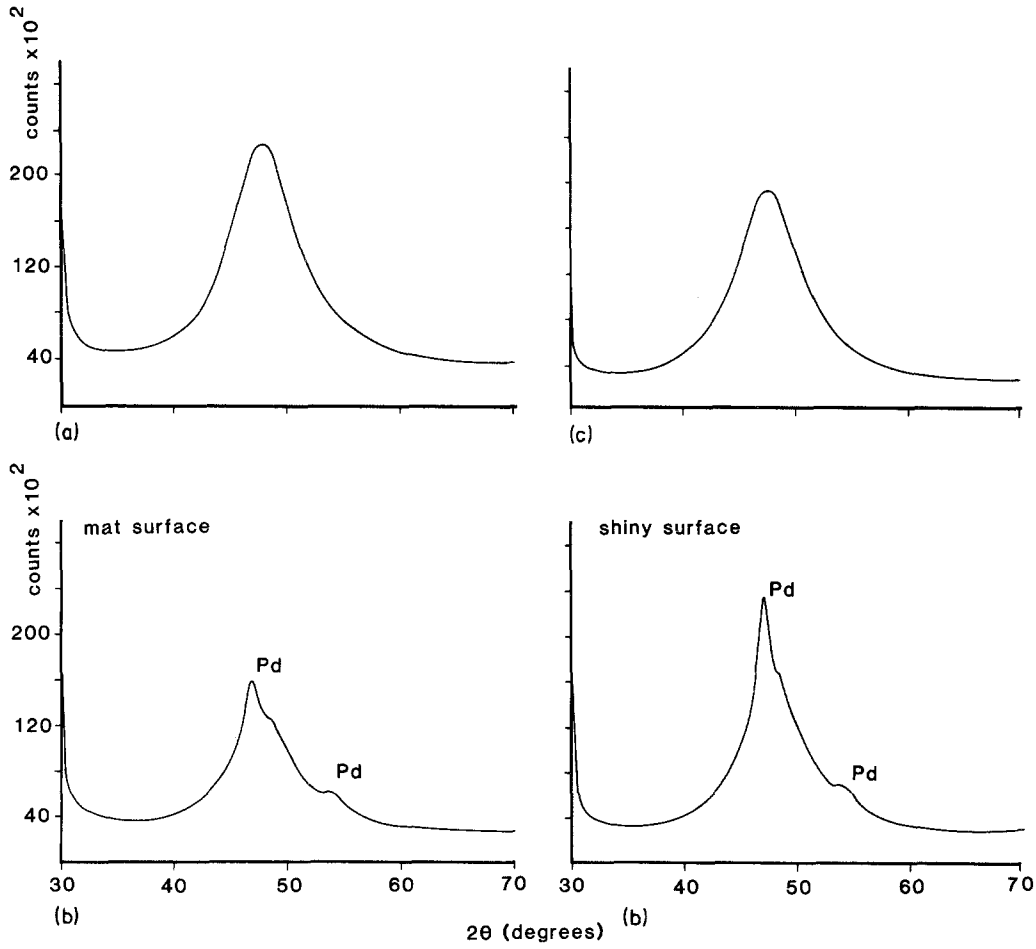

Figure 5 X-ray patterns taken from samples as in Fig. 4 prior to LPC.

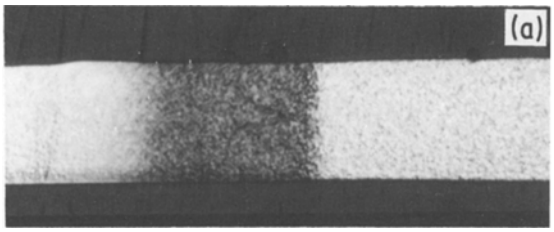

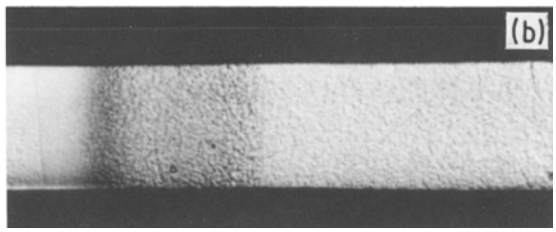

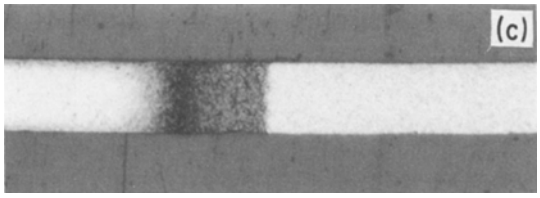

Figure 6 Optical micrographs of LPC crystallized $Pd_{85}Si_{15}$ ribbons. Orientation as in Fig. 2. (a) As-quenched, (b) pre-annealed at 335° C for 5 min, and (c) etched after pre-annealing as in (b).

In the case of LPC of pre-annealed samples, two existing growth processes are apparent (Fig. 4b). Symmetrical growth of columnar crystals from the surface into the bulk is closely followed by bulk nucleation and subsequent growth of cellular crystals. From the observed front profile it is clear that the growth of cellular crystals requires a slightly higher temperature than that of columnar crystals.

The X-ray patterns of pre-annealed samples (Fig. 5b) show generally the same structure as that observed for pre-annealed $Pd_{77}Si_{23}$ samples (amorphous + Pd + traces of the MSI structure). The only difference between them is that for the pre-annealed $Pd_{80}Si_{20}$ samples the peaks corresponding to the MSI phase are less pronounced and the Pd(1 1 1) and Pd(2 0 0) peaks are distinctively stronger.

The LPC front of pre-annealed samples with etched surfaces (Fig. 4c) shows homogeneous crystallization of spherical crystals in the bulk as was observed for as-quenched samples. Corresponding X-ray patterns (Fig. 5c) show only amorphous phase.

3.3. $Pd_{85}Si_{15}$ alloys

The microstructure of the LPC $Pd_{85}Si_{15}$ ribbons (Fig. 6) contains small eutectic cells due to homogeneous crystallization in the bulk. The size of these cells is bigger at shorter distances from the laser-irradiated part of the ribbon, whereas their number is an increasing function of the distance. This picture corresponds to different stages of the kinetics of the crystallization and growth processes captured in one sample. The micrographs do not show a clear border line between amorphous and crystalline phases. The existence of such a dividing region could only be revealed after chemical etching, reflecting the presence of frozen-in high stress concentration areas. As shown in Figs 6a and b, microstructures of the as-quenched, pre-annealed and etched samples are identical despite the fact that the corresponding X-ray patterns indicate strong variation in their surface condition (Fig. 7).

4. Conclusion

Surface crystallization appears to be a characteristic feature of metallic glasses of the metal–metalloid type [3–5]. Understanding of this phenomenon is of great practical importance. Therefore, there is a need for systematic research in this area and, in particular, for developing suitable experimental techniques. In this work, a new method of laser pulse crystallization (LPC) capable of quickly revealing crystallization morphology of metallic glasses has been proposed. This technique enables the study of a crystallization process without simultaneous changing of the properties of the studied sample by its prolonged exposure to elevated temperatures. This is due to its very short characteristic time. This method conveniently supplements X-ray diffractometry and thermal analysis in research on crystallization processes in metallic glasses.

Although the presentation of a detailed model of the dynamics of heat flow in LPC of ribbons goes beyond the scope of this paper, we wish to stress that LPC offers an opportunity to investigate experimentally the kinetics of columnar crystal growth through the general relation:

$$l = \int_{t_1}^{t_2} u[T(t')]\,\mathrm{d}t'$$

where l is a length of the columnar crystals grown, $u(T)$ is the temperature-dependent growth rate, and t_1 and t_2 are the instances when the growth starts and concludes, respectively. The values of t_1 and t_2 should be either measured experimentally or calculated in a heat flow model.

Debye–Scherrer X-ray analysis of tiny ribbon fragments containing crystallization fronts always reveals the existence of the metastable phase II (MSII). The structure of this phase is complicated and not completely recognized. In the region $30° \leqslant 2\theta \leqslant 100°$ all diffraction peaks originally described by Masumoto and Maddin [2] were observed. The presence of MSII in the crystallization front region is independent of either chemical composition of the analysed ribbon or thermal and/or chemical treatment of its surface. It is an unexpected result, indicating that the metastable phase II can be formed in the whole amorphous phase formation region of PdSi system by crystallization processes of various kinetics, and that it can exhibit various morphologies (Figs 2, 4 and 6).

It has been clearly demonstrated that the details of the casting process as well as thermal history affect the surface condition which, in turn, determines the mode of crystallization. Higher stability and lower tendency towards surface crystallization was observed for mat surfaces, which is associated with higher cooling rates for this side of the ribbon. Some of the previously published results demonstrate that, sometimes, the mat surface reveals a stronger tendency towards

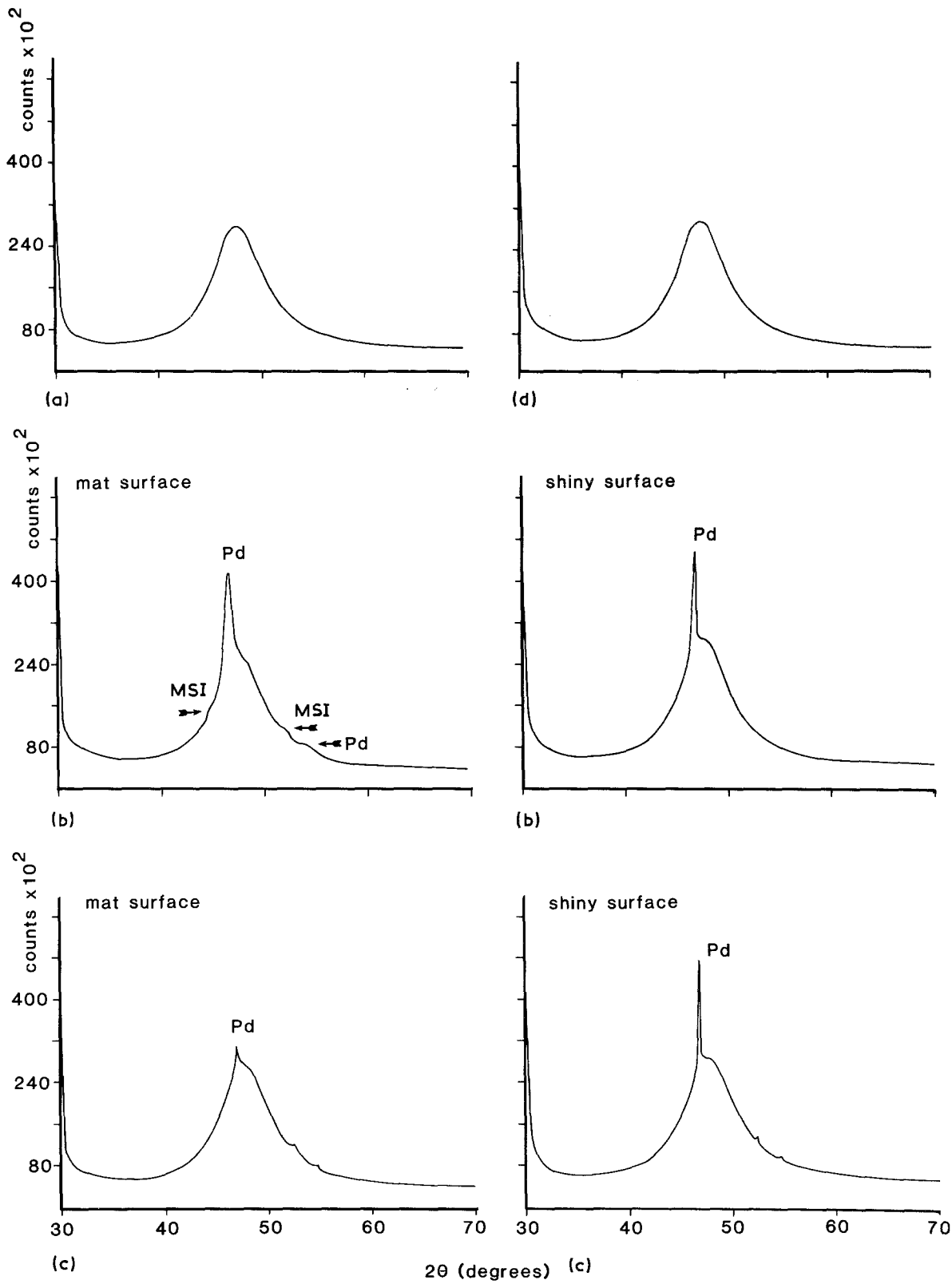

Figure 7 X-ray patterns taken from samples as in Fig. 6 prior to LPC.

surface crystallization [3, 6]. These discrepancies are probably due to varying casting conditions that may influence wetting properties and, as a consequence, good thermal contact between the liquid alloy and spinning wheel. In our work shiny surfaces were systematically more susceptible to surface crystallization than mat surfaces and that trend was more pronounced for thicker ribbons. The surface crystallization studies reported previously were usually conducted on single alloy compositions from different systems. In this work several compositions within the amorphous region of the Pd–Si system were investigated and it was concluded that the influence of the surface on the crystallization mechanism is most pronounced for compositions on the silicon-rich side from the eutectic point. On the other hand, for the eutectic $Pd_{85}Si_{15}$ composition X-ray diffractometry reveals the presence of the surface crystallization, but it appears not to affect the bulk crystallization mechanism.

TABLE I The size of the palladium precipitates in pre-annealed ribbons of several compositions

Ribbon composition	Size of palladium precipitates (nm)	
	Shiny side	Mat side
$Pd_{77}Si_{23}$	5	3
$Pd_{80}Si_{20}$	9	7
$Pd_{85}Si_{15}$	27	12

With a computerized quantitative X-ray diffraction system we were able to produce X-ray patterns of high resolution. The X-ray analysis revealed the existence of precipitated palladium and MSI on the surface. No traces of precipitated silicon were found. This result is consistent with the previous data [4, 7] and indicates that the surface layer is depleted of silicon. Using the the surface layer is depleted of silicon. Using the "ideal" shape of the amorphous peak obtained from etched samples it was possible to separate the signal from the amorphous phase and a crystalline phase due to palladium precipitates. The sizes of crystalline precipitates were determined by applying the well-known Scherrer formula to the diffraction peak corresponding to Pd(1 1 1) (Table I). These results indicate (i) that on annealing under the same conditions the palladium-rich alloys have a stronger tendency towards palladium precipitation and (ii) that those precipitates are always bigger on the shiny surface (which is subject to lower cooling rates) than on the opposite mat surface.

References

1. M. ROSEN, H. N. G. WADLEY and R. MEHRABIAN, *Scripta Metall.* **15** (1981) 1231.
2. T. MASUMOTO and R. MADDIN, *Acta Metall.* **19** (1971) 725.
3. H. G. WAGNER, M. ACKERMANN and U. GONSER, *J. Non-Cryst. Solids* **61/62** (1984) 847.
4. M. MAEDA and M. TANIWAKI, in Proceedings of the 4th International Conference on Rapidly Quenched Metals, Sendai 1981, edited by T. Masumoto and K. Suzuki (Japan Institute of Metals, Sendai, 1982) p. 643.
5. U. KÖSTER, *Z. Metallkd.* **75** (1984) 691.
6. *Idem, Scripta Metall.* **17** (1983) 867.
7. K. TOKUMITSU and H. INO, in Proceedings of the 4th International Conference on Rapidly Quenched Metals, Sendai 1981, edited by T. Masumoto and K. Suzuki (Japan Institute of Metals, Sendai, 1982) p. 647.

Received 25 March
and accepted 11 July 1985